



CONTAINER INFLUENCE ON SHRINKAGE UNDER HOT ISOSTATIC PRESSING—II. SHAPE DISTORTION OF CYLINDRICAL SPECIMENS

E. OLEVSKY

Institute for Mechanics and Materials, University of California, San Diego,
9500 Gilman Drive, La Jolla, CA 92093-0404, U.S.A.

A. MAXIMENKO

Katholieke Universiteit Leuven, Metallurgy and Materials Engineering Department,
de Crylaan 2, Leuven (Heverlee), B-3001, Belgium

(Received 10 December 1996; in revised form 18 June 1997)

Abstract—Finite element modeling of the cylindrical specimen's shape distortion due to the container influence under HIPing is carried out. It is assumed that the mechanical behavior of the powder and the container obeys power law creep equations, and an extremum principle of minimum energy dissipation is taken as the basis of the finite element approach. The specific features of the proposed numerical methods are the utilization of special axisymmetrical shell elements for the container and the iterative approach of the viscous approximations for the solution of the non-linear flow equations. It is noted, that the container influence on the shape change of the specimen depends on the magnitude of the power law creep exponent and distortions are more intensive in the case of low temperature creep. The method for the estimation of the container ribs' influence on the shape deviation is proposed. In many cases, it is possible to produce a precise final shape of the part by the determination of the initial shape of the porous specimen. The iterative method for the prediction of the necessary initial shape is put forward. The method is based on the use of reverse calculations from the final to the initial shape. © 1998 Elsevier Science Ltd. All rights reserved.

1. INTRODUCTION

By convention, one can distinguish two components of the shape change under isostatic pressing. Part I of this paper (Olevsky *et al.*, 1998) is dedicated to the semi-analytical prediction of the *aspect ratio change* of a cylindrical specimen under HIPing, assuming simple kinematic features of the process. However, these calculations carry the germ of the general numerical approach to the problem of the container influence on the specimen shape change. In the general case, any analytical considerations are complicated, but one can get detailed numerical information and determine the main trends of the shape deviation due to the specimen-container interaction.

Shape distortion, including the configuration change when the external surface of a porous specimen loses its cylindricity, is of considerable importance too.

In the present article, the specimen and container are treated as a unified composite porous specimen with a thin outer layer, having mechanical properties different from those in the central part. Full bonding between the container and the specimen is assumed. Two main problems arise in the modeling of such a system. The first specific problem is caused by a considerable dimensional difference between the container and the specimen and the second is a common problem for the modeling of almost all powder metallurgy deformation processes. It lies in the fact that one needs the solution of strongly nonlinear flow problems.

2. FINITE ELEMENT APPROACH IN MODELING OF THE DEFORMATION OF POWDER AND POROUS MATERIALS

The mechanical behavior of any material is considered to be defined, if the constitutive equation is known. This equation relates macroscopic stresses to strains, strain rates and physical parameters of the material. In the case of composite materials, equations can be

derived theoretically if the mechanical properties and geometrical arrangement of the constituents are known. This is relevant, in particular, for porous and powder materials. The macroscopic constitutive equations can be derived using some averaging procedures at the unit cell level. A variety of averaging algorithms enable the solution of this problem. In the theory of nonlinear viscous and plastic behavior of powder and porous materials the dissipation energy method of averaging is commonly used (Kuhn *et al.*, 1993). This method opens considerable possibilities for the development of the finite element method.

The finite element method requires some variational or extremum statement of the problem. If energy dissipation in the material depends only on strain rate tensor components, the dissipation potential Φ can be determined in terms of the average dissipation rate density D (Mosolov and Myasnikov, 1981):

$$\Phi = \int_0^1 D(\alpha e, \alpha \gamma) \frac{d\alpha}{\alpha} \quad (1)$$

where e , γ are the first invariant of the strain rate tensor and the second invariant of the deviator of this tensor, respectively.

The dissipation potential is the main component in the extremum principle for the kinematic parameters of deformation. It was proved by Mosolov and Myasnikov (1981) that velocities of a real deformation process render the minimum for the following functional:

$$I = \int_{\Omega} \Phi \, d\Omega - \int_{\Omega} \mathbf{F} \cdot \mathbf{v} \, d\Omega - \int_S \mathbf{T} \cdot \mathbf{v} \, dS \quad (2)$$

where Ω is the volume of the porous specimen and S is its surface. \mathbf{F} and \mathbf{T} are the body forces and surface traction, respectively and \mathbf{v} is the velocity of the material under deformation.

The precise expression of the average dissipation rate density D can be obtained only as a result of detailed computer calculations. But in our case the following approximation is valid

$$D = \sigma_0 \dot{\epsilon}_0 \sqrt{1-\theta} \left[\frac{\sqrt{\psi e^2 + \varphi \gamma^2}}{\dot{\epsilon}_0} \right]^{\alpha+1} \quad (3)$$

if the skeleton of the porous body obeys power law creep under uniaxial loading

$$\sigma = \sigma_0 \left(\frac{\dot{\epsilon}}{\dot{\epsilon}_0} \right)^{\alpha} \quad (4)$$

where σ , $\dot{\epsilon}$ are axial stress and strain rate, ψ , φ are functions of porosity θ and power law exponent α (Olevsky *et al.*, 1998). Parameter $\dot{\epsilon}_0$ is a constant, determining the time scale of the process and σ_0 is a function of the porous body skeleton's deformation parameters. The generalized Odquist parameter ω is used as a measure of the accumulated skeleton deformation (Olevsky *et al.*, 1998). For the uniaxial loading, ω is equal to the axial deformation and the σ_0 – ω dependence corresponds to the stress–strain relation in this case.

The finite element method provides the numerical approach for the minimization of eqn (2). Using the finite element approximation for the velocity field, we transform expression (2) into a function of unknown nodal velocity values. As a rule, Euler's equation for this function cannot be solved by direct subsequent elimination of unknown parameters. In this case, the iterative method of viscous approximations is appropriate (used by Olevsky

and Maximenko, 1994). The method is based on the approximation of D in the following form :

$$D \approx D_v = \sigma_0 \epsilon_0^{-\alpha} \sqrt{1-\theta} \frac{\psi e^2 - \phi \gamma^2}{(\psi e_0^2 + \phi \gamma_0^2)^{(1-\alpha)/2}} \tag{5}$$

where e_0, γ_0 are taken from the results of the previous iteration. Minimization of D_v requires only the solution of a set of linear equations. It was found by Olevsky and Maximenko (1994) that the proposed iterative scheme always converges to the minimum of the above-mentioned function. If $|e - e_0| \rightarrow 0, |\gamma - \gamma_0| \rightarrow 0$, the right-hand part of eqn (5) is obviously equal to the right-hand part in eqn (3). When the preassigned convergence criterion is stringent enough, the accuracy of the minimization eqn (2) depends only on the finite element mesh specification.

3. GEOMETRICAL ASPECTS OF THE FINITE ELEMENT MODELING FOR HOT ISOSTATIC PRESSING

Typically, one of the specific dimensions of the container is considerably smaller than the average size of the porous specimen. Engineers often try to make container walls as thin as possible in order to decrease waste product and to preserve the semblance of the initial and final shapes of the part.

Dimensional differences can be ignored in the calculations only in the case when the average size of the cells of the mesh for the porous specimen is comparable to the container wall thickness. Modern computer facilities allow this type of numerical approach used by Abouaf *et al.* (1988) and Nohara *et al.* (1988), but the shape change prediction is possible in a much easier way (which substantially decreases computation time) with the use of a coarse mesh for the part and specific finite elements for the container.

The direct application of the coarse mesh throughout the whole composite porous specimen causes difficulties, because the distance between nodes in the container volume must be small. It is known, that the velocity field is poorly defined by two nodal velocities which are close to each other. The velocity components which are normal to the surface of the part become almost equal in the calculations and that leads to linear dependence in the total velocity vector and, consequently, to an ill-conditioned matrix of equations (see, for example, A Finite Element Primer (1986)).

One possible way to get rid of these troubles is the use of special shell elements. The main idea of the shell elements is the abandonment of the nodal velocities as unknown values in the Euler equation for the functional (2).

The topology of the proposed axisymmetrical shell element is shown in Fig. 1. For each viscous approximation D_v , velocities at the central node of elements are determined

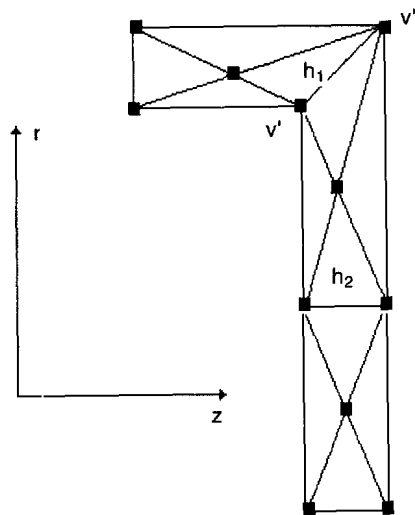


Fig. 1. Topology of the container meshing.

as functions of the other nodal velocity values by proper minimization of eqn (2). Therefore, the contribution of each element to the global set of equations depends only on the velocities in the corners of elements.

Integration of eqn (5) over any container element gives the following quadratic contribution to the approximation of the functional

$$\Delta I = C_{ij}v_i v_j \quad i = \overline{1,8}; \quad j = \overline{1,8} \quad (6)$$

where v_i are velocity components. Let us assume that the first four indices in C_{ij} correspond to the velocities \mathbf{v}' at the internal surface of the container, and the other four stand for the components of velocities \mathbf{v}'' at the outer surface. The indices of the respective components of the velocities at the opposite sides of the container differ by four.

Let us introduce the following representation for the nodal velocities in the container volume

$$\mathbf{v}'' = \mathbf{v}' + \xi \delta \quad (7)$$

where δ is the container thickness. The parameters ξ are considered as new unknown values and eqn (7) is the rule of transformation from \mathbf{v}'' to ξ . In the simplest case considered by Olevsky *et al.* (1998), eqn (7) defines a transformation from the nodal velocities to the strain rate tensor components. Substitution of eqn (7) into the set of equations with respect to velocities eliminates terms of order $1/\delta$ and improves the matrix condition.

Replacement of the velocities \mathbf{v}'' at the external surface of the container by ξ can be carried out as a transformation of the matrix C_{ij}

$$\hat{C}_{ij} = T_{ik} C_{kl} T_{lj} \quad (8)$$

where \hat{C}_{ij} specifies ΔI eqn (6) as a function of the components of \mathbf{v}' , ξ . The non-zero entries of the matrix T_{ij} can be given in the following form

$$\begin{aligned} T_{ii} = T_{i,i+4} = 1 \quad i = \overline{1,4} \\ T_{i+4,i+4} = \begin{cases} h_1, & i = 1, 2 \\ h_2, & i = 3, 4 \end{cases} \end{aligned} \quad (9)$$

where parameters h_1, h_2 are shown in Fig. 1.

The proposed transformation allows the consideration of container elements with arbitrary thickness and enables us to trace the container influence as $\delta \rightarrow 0$. The shape change must be completely absent for $\delta \approx 0$.

4. THE MAIN REASONS OF THE CONTAINER INFLUENCE ON THE SHAPE DISTORTION UNDER HIP

At high temperatures materials show a rate dependent mechanical behavior or creep. Above $0.3-0.4T_m$, stress-strain rate equations can be expressed in the form of a power law used by Frost and Ashby (1982) (T_m is a melting point). The microscopic mechanism of creep is changed when temperature increases. At lower temperatures ($<0.6T_m$), the so-called low temperature creep is noted and above this temperature the mechanism is changed into high-temperature creep. The exponent α_{LT} from the relationship (4) in the case of low temperature creep is smaller than the exponent α_{HT} for high temperature creep. A simple empirical rule is introduced by Frost and Ashby (1982):

$$\frac{1}{\alpha_{LT}} = \frac{1}{\alpha_{HT}} + 2 \quad (10)$$

At the temperatures below $0.3T_m$, the main mechanism of material flow is the low-temperature plasticity and if the yield strength of material does not depend on the strain rate, the exponent α is equal to zero.

It turns out, that variations of the strain rate exponents in the vicinity of zero considerably impact the deformation behavior of materials under HIPing. The deformation of a nickel powder cylinder in a stainless steel container was considered as a model problem. The rate exponent for nickel changes from 0.14 to 0.22 when the temperature increases and the same parameter for steel lies in the range between 0.1 and 0.12 in accordance with the data of Frost and Ashby (1982). HIPing at temperatures 600 and 1100 K was simulated. Functions $\sigma_0 - \omega$ for the above-mentioned materials were taken as polynomial approximations of the pertinent stress-strain curves from the reference book of Poluhin *et al.* (1983). These approximations are given in the Appendix. The material of the container is treated as incompressible and the initial porosity of the nickel was 0.4 in all the cases. In the modeling, the external pressure was held equal to the all-round compaction yield limit of the nickel powder

$$P = \sigma_0 \sqrt{(1-\theta)\psi} \quad (11)$$

The external pressure was treated according to Olevsky *et al.* (1998).

The time of the model HIPing was not constrained. Calculations in every case were performed until the average porosity of the compact met the value 0.5%. This type of modeling provided a way of correct shape change comparison in the different cases.

A comparison of the shape evolution at the different temperatures is given in Fig. 2a ($T = 600$ K) and Fig. 2b ($T = 1100$ K). The initial ratio of the container thickness and the diameter of the specimen was taken as 0.04 to provide detectable shape change for the pictures.

It is obvious (Fig. 2) that high temperature creep is associated with considerably smaller shape deviations. The explanations of this effect become more clear in the case of contrasting porosity distributions in both cases (Fig. 3). The porosity gradients during low temperature creep are more steep than for high temperature creep because internal homogenization of porosity is hindered due to the small power law exponent. Internal redistribution of porosity is favorable for a more uniform pressing of the part. Porosity distributions in Fig. 3 correspond to the moment, when average volume porosities were equal to 0.1 in both cases.

The influence of the container on the final shape of the part depends also on the rigidness of the container ribs. If the shell thickness is less than 1% of its other specific dimensions, the influence of the shell joints is believed to be insignificant in the theory of elastic shells (Abouaf *et al.*, 1988). Under pressing, the contributions of the container ribs into shape deviations are accumulated during the whole course of the process and the result depends not only on the aspect ratio of the shell, but also on the total deformation of the part.

A precise element investigation of the container ribs' influence necessitates special meshing. As a result, it gives rise to additional cumbersome calculations. The most simple way of solving this problem is the use of constraint equations at the corners of the container. The two extreme conditions are: (i) velocity continuity without any limitation on the evolution of the container angles; (ii) rigid joints at the corners. The difference between these two cases can be considered as a measure of the ribs impact on the shape deviation of the specimen (Fig. 4).

If the shape deviation due to the container influence exceeds the required tolerance for the part, the following question arises: how the initial shape of the porous specimen should be changed to provide an accurate final configuration. The answer to this question can be given by an iterative procedure based upon the repeated "direct" and "reverse" calculations

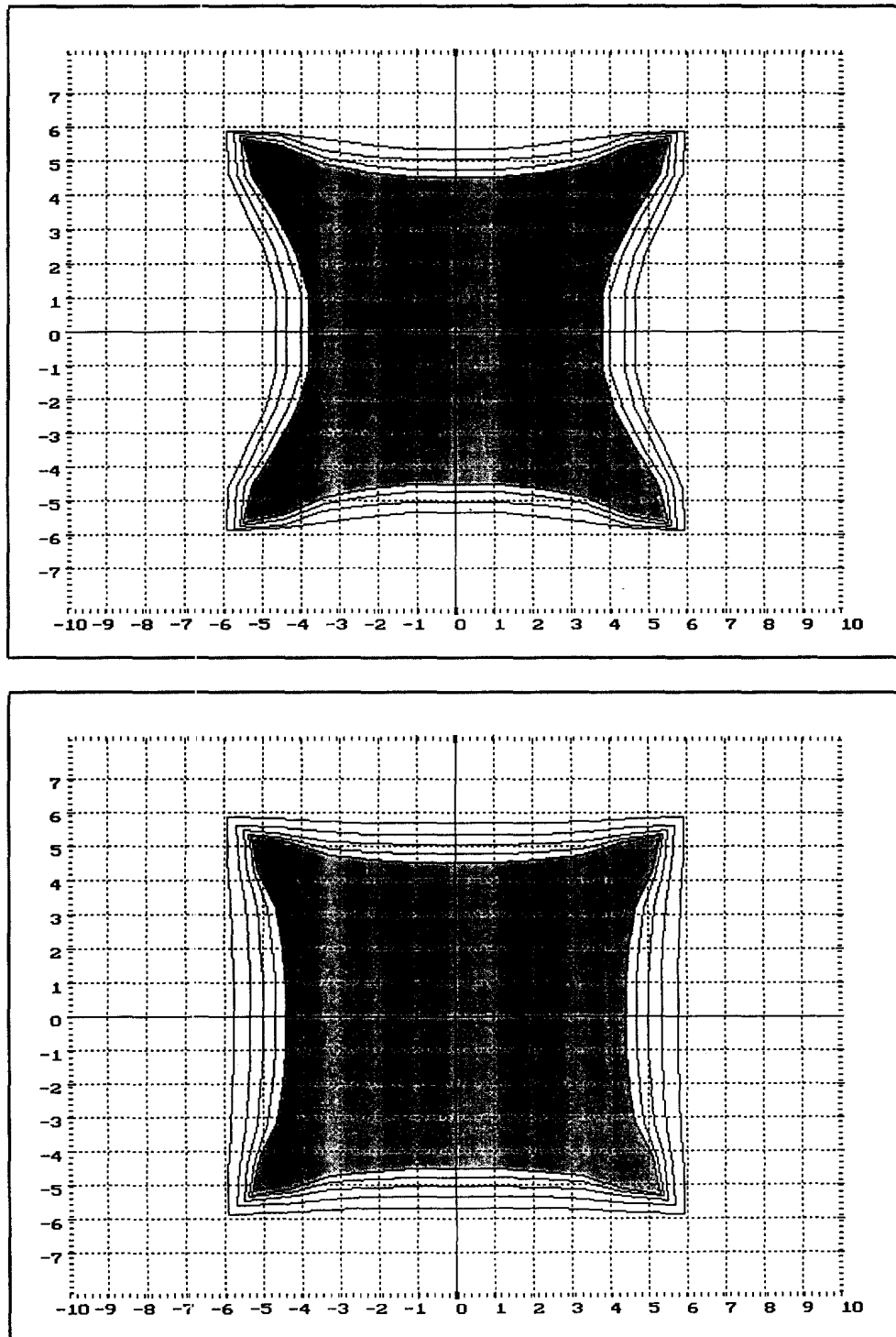


Fig. 2. The influence of the temperature on the shape change of the cylindrical specimen: (a) $T = 600$ K; (b) $T = 100$ K.


of the shape change. If the final shape of the part is known, one can consider an expansion of the final shape to the initial shape of the porous specimen introducing the pressure which is equal to the given external pressure, however, applied in an opposite direction (tensile load instead of compression). The law of material hardening due to the accumulated deformation of the powder skeleton must be also taken in the "reverse" direction as the law of softening.

porosity

0.078 .. 0.082

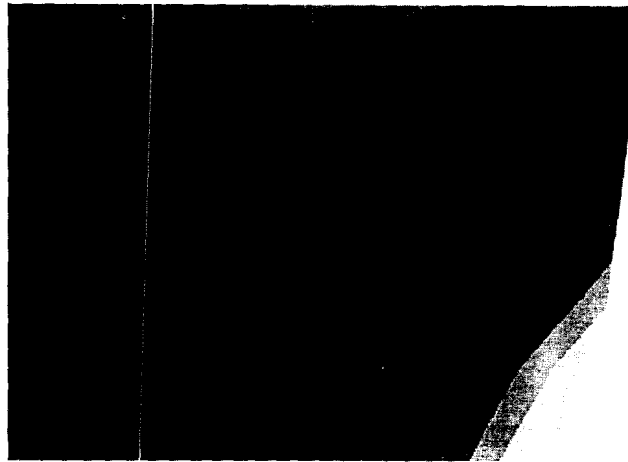
0.082 .. 0.086

 0.086 .. 0.091

 0.091 .. 0.095


 0.095 .. 0.099


 0.099 .. 0.103





porosity

0.097 .. 0.100

 0.100 .. 0.103

 0.103 .. 0.105

 0.105 .. 0.108

 0.108 .. 0.111


 0.111 .. 0.113



Fig. 3. Porosity distributions for different pressing temperatures : (a) $T = 600$ K ; (b) $T = 1100$ K.

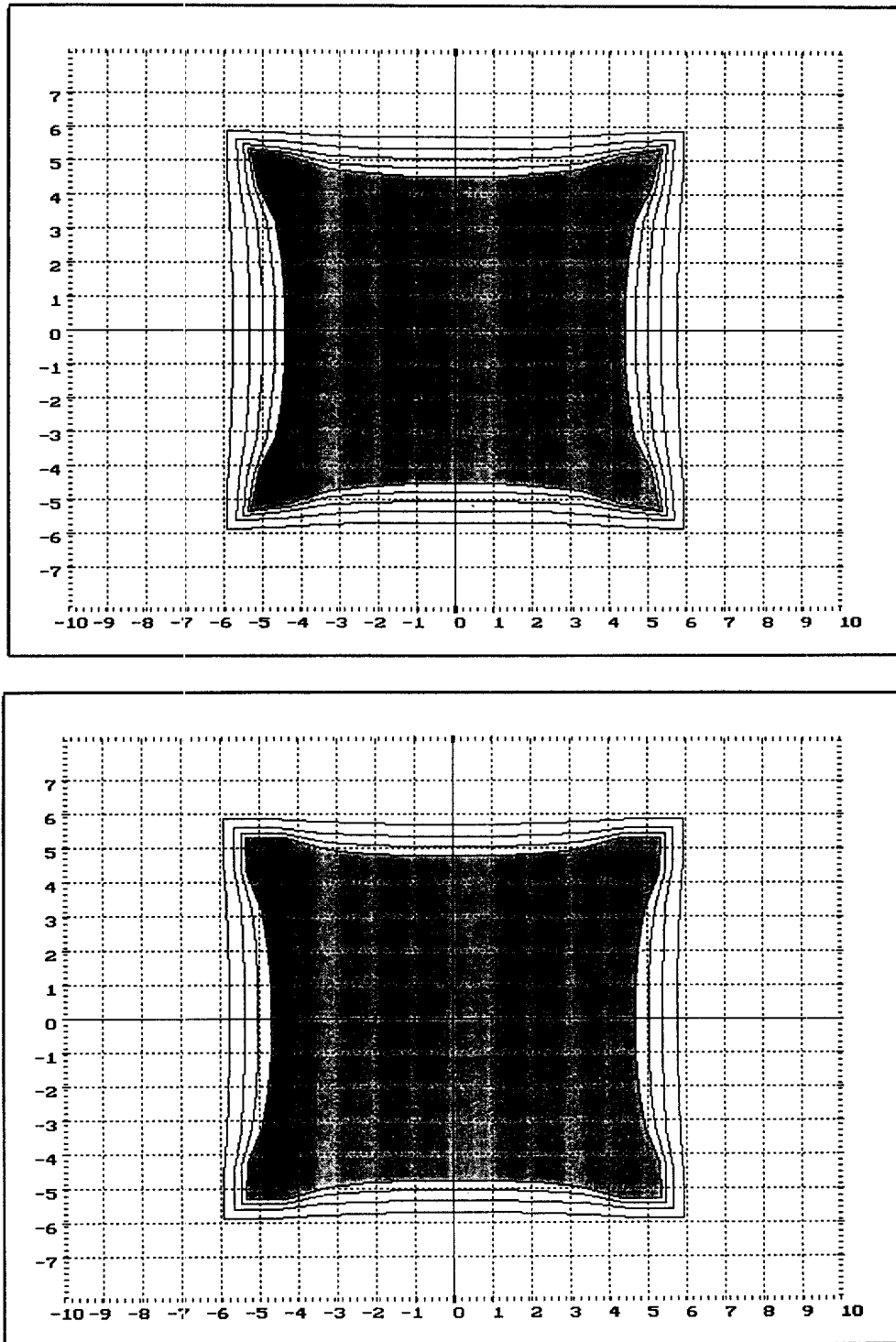


Fig. 4. The influence of the rigidity of the container ribs: (a) free hinges at the corners; (b) rigid joint at the corners.

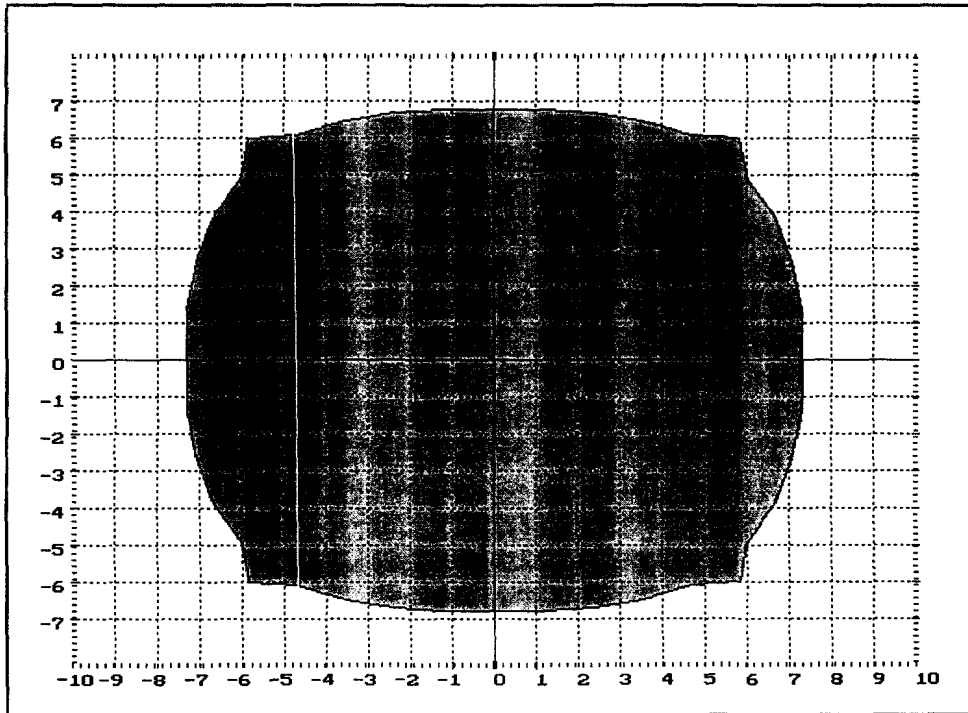


Fig. 5. Calculated initial shape of the workpiece for the cylindrical part.

At the first iteration, we take the initial shape of the porous specimen completely similar to the final shape of the part and realize the first "direct" calculation to the final shape. Then we transform obtained shape into the required final shape by changing every node coordinate according to the rule:

$$\begin{aligned} z &= z_i \sqrt[3]{\frac{V_f}{V_i}} \\ r &= r_i \sqrt[3]{\frac{V_f}{V_i}} \end{aligned} \quad (12)$$

where z_i , r_i are the initial node coordinates and V_f , V_i are the final and the initial volumes of the porous specimen, respectively. Porosity and Odquist parameter distributions over the finite elements remain unchanged.

The next step is a "reverse" movement from the final to the new initial shape. This initial shape is different from the shape at the first iteration and, in general, the porosity and Odquist parameter are nonuniform in the volume of the new initial shape. Hence, we take the calculated shape as the shape for the second iteration, but assume a uniform distribution of the preassigned porosity and accumulated deformation values in the volume. Then we can repeat all procedures from the very beginning. It should be noted that transformations (12) are the same for all iterations.

It is very difficult to justify rigorously the convergence of the proposed approach, but as a rule, two or three iterations always allow the choice of the necessary initial shape (which can be proved by "direct" calculations). The initial shape for the cylindrical specimen in the case of pressing at the temperature 600 K and initial porosity 0.4 is given in Fig. 5.

5. CONCLUSIONS

The container influence is the main origin of the regular shape change during HIPing. In general, shape distortion is a result of the container-powder mechanical property difference and the nonuniform rigidity of the container.

The extent of the container impact on the shape distortion is considerably sensitive to the magnitude of the power law creep exponent and, consequently, to the type and physical mechanism of the creep. At low temperature, the shape change is more intensive due to the arising substantial density nonuniformity of the specimen during pressing. In this case, the precise final shape of the part can be obtained by the predetermined variations of the initial shape.

Acknowledgements—Drs Olevsky and Maximenko acknowledge a Research Fellowship of the Katholieke Universiteit Leuven. The support of Dr Olevsky by the NSF Institute for Mechanics and Materials, University of California, San Diego is gratefully acknowledged.

REFERENCES

- Abouaf, M., Chenot, J. L., Raisson, G. and Bauduin, P. (1988). Finite element simulation of hot isostatic pressing of metal powders. *International Journal of Numerical Methods in Engineering* **25**(1), 191–212.
- A Finite Element Primer* (1986). National Agency for Finite Element Methods & Standards, Glasgow.
- Frost, H. J. and Ashby, M. F. (1982). *Deformation-Mechanism Maps*, Pergamon Press, New York.
- Kuhn, L., Xu, J. and McMeeking, R. (1993). Constitutive models for the deformation of powder compacts. In *Computational & Numerical Techniques in Powder Metallurgy* (Edited by D. Madan, I. Anderson, W. Fraizer, P. Kumar and M. McKimpson), pp. 123–136. The Mineral, Metals & Materials Society.
- Mosolov, P. P. and Myasnikov, V. P. (1981). *Mechanics of Rigid-Plastic Media*, Nauka, Moscow.
- Nohara, A., Nakagawa, T., Soh, T. and Shinke, T. (1988). Numerical simulation of the densification behaviour of metal powder during hot isostatic pressing. *International Journal of Numerical Methods in Engineering* **25**(1), 213–225.
- Olevsky, E. and Maximenko, A. (1994). Nonstationary problems of the quasistatic theory of hardening plastic bodies. *Computational Materials Science* **3**, 247–253.
- Olevsky, E. *et al.* (1998) Container influence on shrinkage under hot isostatic pressing—I. Shrinkage anisotropy of a cylindrical specimen. *International Journal of Solids and Structures* **35**, 2283–2303.
- Poluhin, P. I., Gun, G. Ya. and Galkin, A. M. (1983). Plastic deformation of metals and alloys. *Metallurgia*, Moscow (in Russian).

APPENDIX

The law of hardening for nickel (σ_0 has the units of MPa):

$$\begin{aligned}\sigma_0 &= 102.9 + 1793\omega - 1099\omega^2 & T = 600 \text{ K} \\ \sigma_0 &= 82.9 + 1690\omega - 993\omega^2 & T = 1100 \text{ K}\end{aligned}$$

The law of hardening for stainless steel:

$$\sigma_0 = 188 + 1081\omega - 1614\omega^2$$